Micro Scale Modeling of Grain Boundary Damage under Creep Conditions

Oksana Ozhoga-Maslovskaja
Supervisors: Holm Altenbach, Konstantin Naumenko, Manja Krüger

Experimental Observation

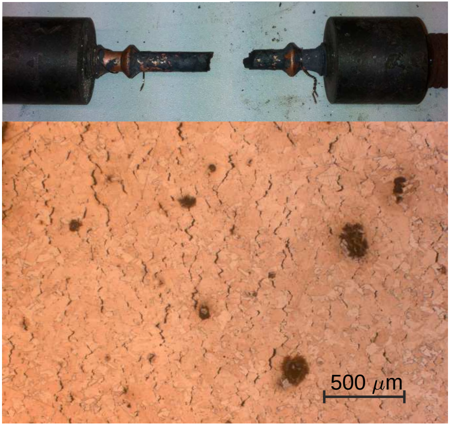

Creep fracture at different scales: fractured creep specimen, micrograph of the copper specimen, tested at 550 °C and 25 MPa

Creep Fracture

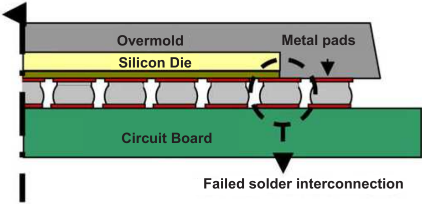

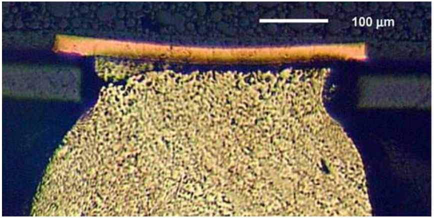

Typical crack through solder joint interface. Scheme of solder interconnection in an electronic assembly (Towashiraporn et al., 2005)

Creep in a Polycrystalline Solid [1]

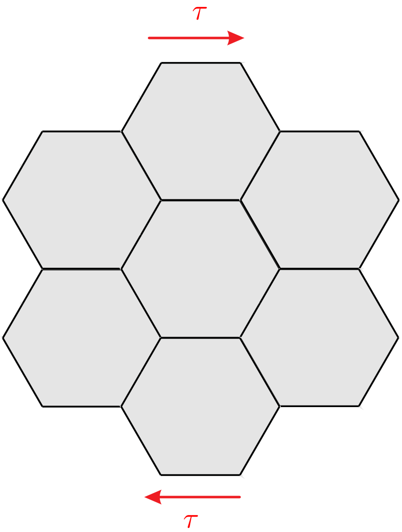

- Elastic stress concentration;
- Plastic flow-field;
- Diffusive flow-field of matter;
- Cavity formation in triple points and at grain boundaries.

[1] Crossman and Ashby, 1975

Creep in a Polycrystalline Solid [1]

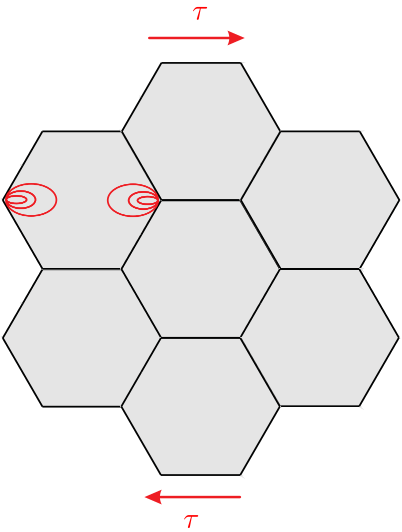

- Elastic stress concentration;
- Plastic flow-field;
- Diffusive flow-field of matter;
- Cavity formation in triple points and at grain boundaries.

[1] Crossman and Ashby, 1975

Creep in a Polycrystalline Solid [1]

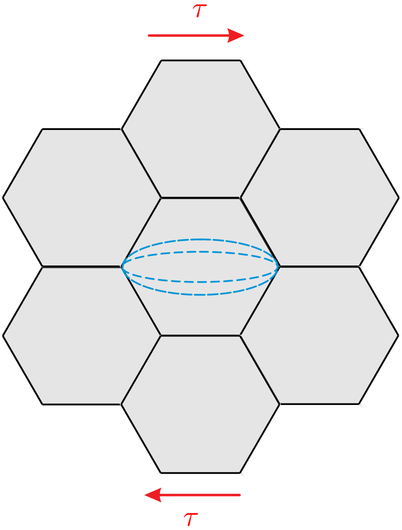

- Elastic stress concentration;
- Plastic flow-field;
- Diffusive flow-field of matter;
- Cavity formation in triple points and at grain boundaries.

[1] Crossman and Ashby, 1975

Creep in a Polycrystalline Solid [1]

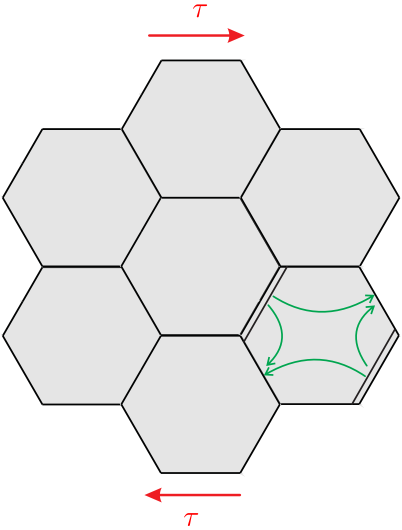

- Elastic stress concentration;
- Plastic flow-field;
- Diffusive flow-field of matter;
- Cavity formation in triple points and at grain boundaries.

[1] Crossman and Ashby, 1975

Creep in a Polycrystalline Solid [1]

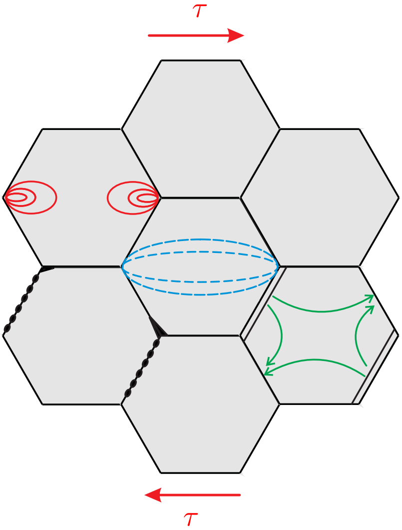

- Elastic stress concentration;
- Plastic flow-field;
- Diffusive flow-field of matter;
- Cavity formation in triple points and at grain boundaries.

[1] Crossman and Ashby, 1975

Idea of the Study

Aim of the Study

To perform creep damage analysis of the polycrystalline material on the micro scale in order to investigate the influence of chosen micromechanisms on the creep curve of meso–material

Considered mechanisms

- Elastic deformation of anisotropic grains;
- Power law creep;
- Grain boundary sliding;
- Grain boundary cavitation (Tvergaard 1984);
- Stiffness reduction due to cavitation.

Other mechanisms

- Dislocations and vacancies movement;
- Dislocation pile ups;
- Subgrains and slip bands formation.

Collaboration

Polycrystalline geometry:

- Oleksandr Prygorniev "Micromechanical simulation of deformation and fatigue of polycrystalline materials";
- Srihari Dodla "Experimental and numerical investigations of lamellar copper silver composites".

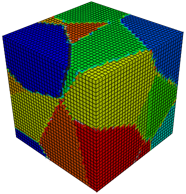

Similar field researches:

- Shyamal Roy, Esmaeil Tohidlou, Dr.–Ing. Rainer Glüge.

Collaboration

- The uniaxial tensile creep tests under polycrystalline copper at 550 °C are performed in order to observe the micromechanisms taking place during creep.

Prof. Gariboldi
Dipartimento di Meccanica
Politecnico di Milano
Italia

- Micrographs of the fractured specimens are performed with Jun.-Prof. Dr.-Ing. Manja Krüger assistance.

Geometrical Model of Polycrystal

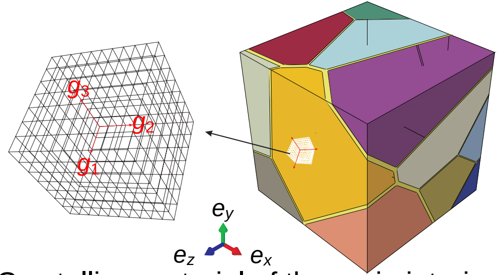

Crystalline material of the grain interior

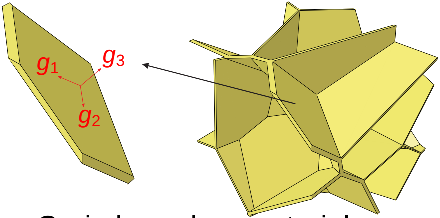

Grain boundary material

Linear Elasticity

Elasticity law

$$
\begin{aligned}
\boldsymbol{\sigma} &= \alpha_1^2(\varepsilon_{11}+\varepsilon_{22}+\varepsilon_{33})(\boldsymbol{g}_1\otimes\boldsymbol{g}_1+\boldsymbol{g}_2\otimes\boldsymbol{g}_2+\boldsymbol{g}_3\otimes\boldsymbol{g}_3)\\
&+ [\beta_1(\varepsilon_{11}-\varepsilon_{22})+\beta_2(\varepsilon_{11}-\varepsilon_{33})]\boldsymbol{g}_1\otimes\boldsymbol{g}_1+[\beta_1(\varepsilon_{22}-\varepsilon_{11})+\beta_3(\varepsilon_{22}-\varepsilon_{33})]\boldsymbol{g}_2\otimes\boldsymbol{g}_2\\
&+ [\beta_2(\varepsilon_{33}-\varepsilon_{11})+\beta_3(\varepsilon_{33}-\varepsilon_{22})]\boldsymbol{g}_3\otimes\boldsymbol{g}_3+2\beta_{12}\varepsilon_{12}(\boldsymbol{g}_1\otimes\boldsymbol{g}_2+\boldsymbol{g}_2\otimes\boldsymbol{g}_1)\\
&+ 2\beta_{13}\varepsilon_{13}(\boldsymbol{g}_1\otimes\boldsymbol{g}_3+\boldsymbol{g}_3\otimes\boldsymbol{g}_1)+2\beta_{23}\varepsilon_{23}(\boldsymbol{g}_2\otimes\boldsymbol{g}_3+\boldsymbol{g}_3\otimes\boldsymbol{g}_2)
\end{aligned}
$$

Grain interior

$$\alpha_1^2 = 125\ \text{GPa}^a$$
$$\beta_1 = \beta_2 = \beta_3 = 12.3\ \text{GPa}$$
$$\beta_{12} = \beta_{13} = \beta_{23} = 62.3\ \text{GPa}$$

[a] Chang and Himmel, 1966

Grain boundary

$$\alpha_1^2 = 600\ \text{GPa}$$
$$\beta_1 = \beta_2 = \beta_3 = 12.3\ \text{GPa}$$
$$\beta_{12} = \beta_{13} = \beta_{23} = 62.3\ \text{GPa}$$

Creep Behavior

Creep strain rate evolution equation

$$
\begin{aligned}
\dot{\varepsilon}^{c} &= \frac{1}{2} a \sigma_{eq}^{n-1} \left\{ \left[\mu_1(\sigma_{11} - \sigma_{22}) + \mu_3(\sigma_{11} - \sigma_{33}) \right] \left(\boldsymbol{g}_1 \otimes \boldsymbol{g}_1 - \frac{1}{3}\boldsymbol{I} \right) \right. \\
&+ \left[\mu_2(\sigma_{22} - \sigma_{33}) + \mu_1(\sigma_{22} - \sigma_{11}) \right] \left(\boldsymbol{g}_2 \otimes \boldsymbol{g}_2 - \frac{1}{3}\boldsymbol{I} \right) \\
&+ \left[\mu_3(\sigma_{33} - \sigma_{11}) + \mu_2(\sigma_{33} - \sigma_{22}) \right] \left(\boldsymbol{g}_3 \otimes \boldsymbol{g}_3 - \frac{1}{3}\boldsymbol{I} \right) + 6 \left[\mu_{12}\tau_{12}(\boldsymbol{g}_1 \otimes \boldsymbol{g}_2 + \boldsymbol{g}_2 \otimes \boldsymbol{g}_1) \right. \\
&+ \left. \left. \mu_{13}\tau_{13}(\boldsymbol{g}_1 \otimes \boldsymbol{g}_3 + \boldsymbol{g}_3 \otimes \boldsymbol{g}_1) + \mu_{23}\tau_{23}(\boldsymbol{g}_2 \otimes \boldsymbol{g}_3 + \boldsymbol{g}_3 \otimes \boldsymbol{g}_2) \right] \right\}
\end{aligned}
$$

Equivalent stress

$$
\begin{aligned}
\sigma_{eq}^2 &= \frac{1}{2} \left[\mu_1 (\sigma_{11} - \sigma_{22})^2 + \mu_2 (\sigma_{22} - \sigma_{33})^2 + \mu_3 (\sigma_{33} - \sigma_{11})^2 \right] \\
&+ 3 \left[\mu_{12}\tau_{12}^2 + \mu_{23}\tau_{23}^2 + \mu_{13}\tau_{13}^2 \right]
\end{aligned}
$$

Material Parameters Identification

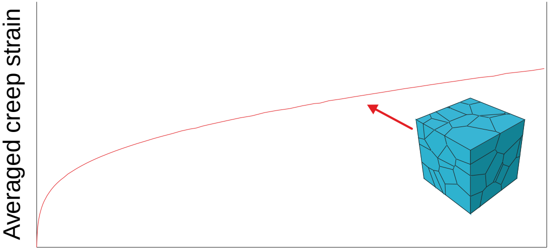

Idea of the numerical test

Material model parameters

Parameter	Grain interior	Grain boundary
$A, \frac{(\mathrm{MPa})^{-n}}{\mathrm{s}}$	$4 \cdot 10^{-15}$	$6 \cdot 10^{-8}$
n	9.4	4
μ_1, μ_2, μ_3	1	0.2
$\mu_{12}, \mu_{23}, \mu_{13}$	0.2	0.3

Material Parameters Identification

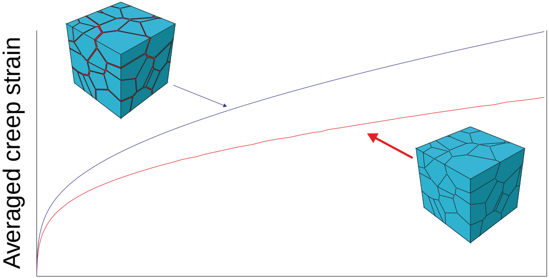

Idea of the numerical test

Material model parameters

Parameter	Grain interior	Grain boundary
A, $\frac{(\mathrm{MPa})^{-n}}{\mathrm{s}}$	$4 \cdot 10^{-15}$	$6 \cdot 10^{-8}$
n	9.4	4
μ_1, μ_2, μ_3	1	0.2
$\mu_{12}, \mu_{23}, \mu_{13}$	0.2	0.3

Material Parameters Identification

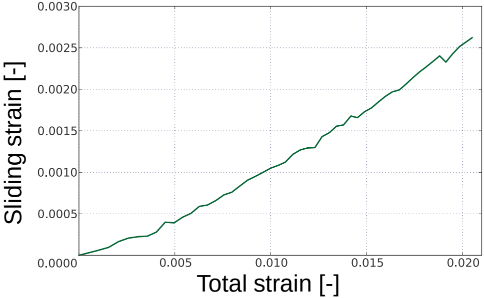

Sliding strain in the loading direction

Material model parameters

Parameter	Grain interior	Grain boundary
A, $\frac{(\mathrm{MPa})^{-n}}{\mathrm{s}}$	$4 \cdot 10^{-15}$	$6 \cdot 10^{-8}$
n	9.4	4
μ_1, μ_2, μ_3	1	0.2
$\mu_{12}, \mu_{23}, \mu_{13}$	0.2	0.3

Model Application

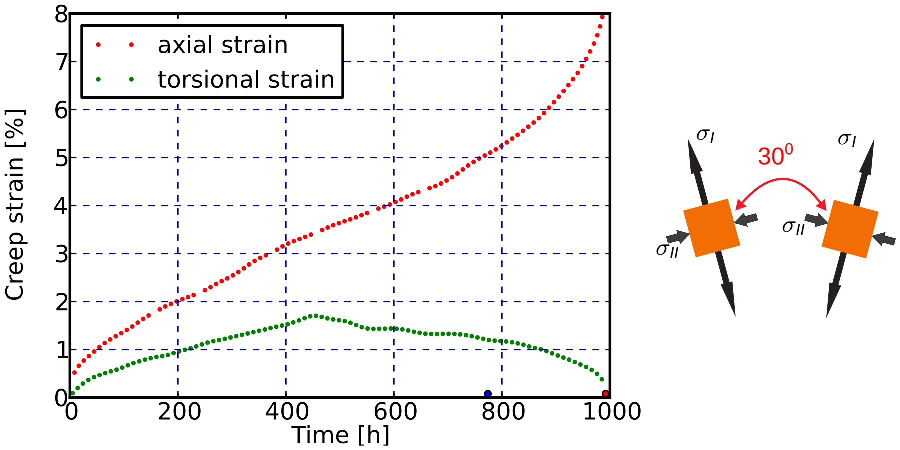

Creep curves of the axial and torsional strains of the non-proportional loading tests of Murakami and Sanomura (1985) with the principal stress direction rotation at 30°

Model Application

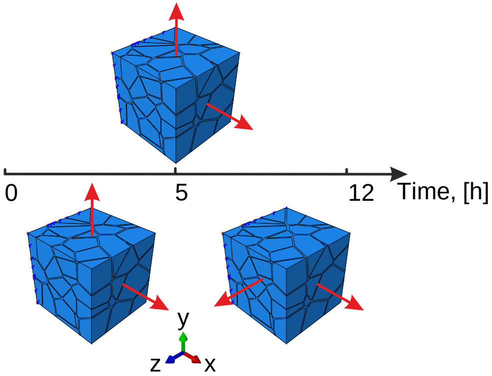

Non-proportional loading			Proportional loading		
Loading direction	Stress, [MPa]	Time, [h]	Loading direction	Stress, [MPa]	Time, [h]
x	30	0–12	x	30	0–12
y	15	0–5	y	15	0–12
z	15	5–12	z	15	——

Model Application

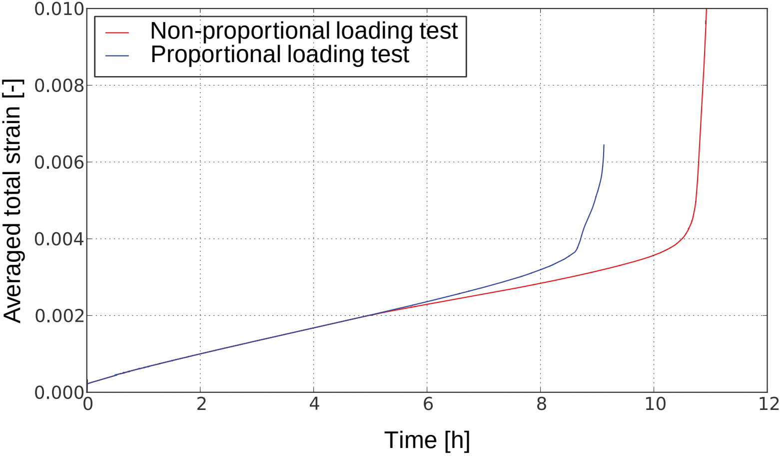

Evolution of the total strain in the x–direction with time for the case of proportional and non–proportional loading cases

Model Application

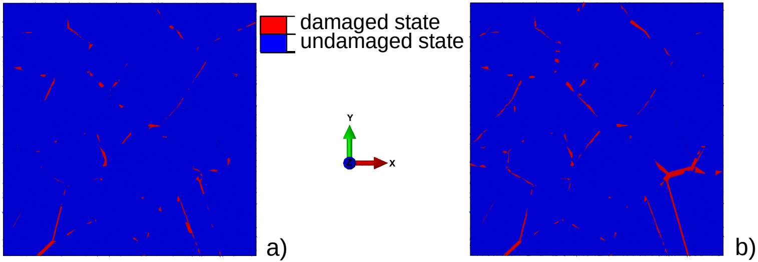

Distribution of damage in the cross–section of the unit cell after 9 hours of creep testing under a) non–proportional loading and b) proportional loading

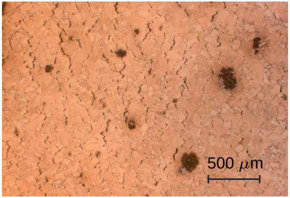

Copper microstructure after creep testing at 25 MPa

Summary

- The copper microstructure is simulated by means of the unit cell.
- The material model parameters are determined from the elastic and creep tensile tests on the single crystal copper.
- The grain boundary sliding is validated by means of the experimental data.
- The creep cavitation and stiffness reduction models are implemented to introduce the tertiary creep stage.
- The developed model is able to reflect the following phenomena observed on the averaged creep curve of the unit cell, tested under non–proportional loading test:
    - On the averaged strain diagram the strain rate decrease is detected after the principal axes rotation;
    - On the cross–sectional diagram of the unit cell the cavitation of the grain boundaries orthogonal to the maximum principal stress is noticed;
    - The prolongation of the time to rupture for the non-proportional loading case is observed. This can be explained by the fact, that after the principal axes rotation another grain boundaries are involved in the cavitation process.

Thank You for attention!